1   **Anatomy of an Extensively Drug Resistant *Klebsiella pneumoniae* Outbreak in Tuscany,**

2   **Italy**

3   Melissa J. Martin[a], Brendan W. Corey[a], Filomena Sannio[b], Lindsey R. Hall[a], Ulrike

4   MacDonald[c,d], Brendan T. Jones[a], Emma G. Mills[a], Jason Stam[a], Rosslyn Maybank[a], Yoon

5   Kwak[a], Katharina Schaufler[g], Karsten Becker[h], Nils-Olaf Hübner[i], Stefania Cresti[b,j], Giacinta

6   Tordini[b,j], Marcello Valassina[j], Maria Grazia Cusi[b,j], Jason W. Bennett[a], Thomas A. Russo[c,d,e,f],

7   Patrick T. McGann[a], Francois Lebreton[a,1*] and Jean-Denis Docquier[b,k,1*]

8   [a]Multidrug-Resistant Organism Repository and Surveillance Network (MRSN), Walter Reed

9   Army Institute of Research, Silver Spring, Maryland, USA

10   [b]Dipartimento di Biotecnologie Mediche, University of Siena, I-53100, Siena, Italy

11   [c]Veterans Administration Western New York Healthcare System; [d]Department of Medicine;

12   [e]Department of Microbiology and Immunology; [f]The Witebsky Center for Microbial

13   Pathogenesis; University at Buffalo, State University of New York, Buffalo, New York, USA

14   [g]Institute of Pharmacy, Pharmaceutical Microbiology, University of Greifswald. [h]Friedrich

15   Loeffler-Institute of Medical Microbiology and [i]Central Unit for Infection Prevention and

16   Control, University Medicine Greifswald, Greifswald, Germany.

17   [j]UOC Microbiologia e Virologia, Azienda Ospedaliera Universitaria Senese, I-53100, Siena,

18   Italy.

19   [k]Centre d'Ingénierie des Protéines-InBioS, Université de Liège, B-4000 Liège, Belgium.

20   *To whom correspondence may be addressed. Email: francois.lebreton.ctr@mail.mil or

21   jddocquier@unisi.it

22   [1]F.L. and J-D.D. contributed equally to this work.

23   **Author Contributions:** J.W.B., P.T.M., F.L. and J-D.D. designed research; M.J.M., B.W.C.,

24   F.S., L.R.H., U.M., B.T.J., E.G.M., J.S., R.M., Y.K., T.A.R and F.L. performed research.

25   M.J.M., B.W.C., F.S., L.R.H., U.M., B.T.J., E.G.M., J.S., K.S., T.A.R, P.T.M, F.L. and J-D.D.

26   analyzed research; F.S., K.S., K.B., N-O.H., S.C., G.T., M.V., M.G.C and J-D.D. contributed

27   clinical metadata and isolates. M.J.M. and F.L. wrote the paper with inputs from all authors.

28   **Competing Interest Statement:** The authors declare no competing interest.

29   **Classification:** Biological sciences, Microbiology.

30   **Keywords:** Antimicrobial resistance, virulence, genomic epidemiology, nosocomial infection

Abstract

A protracted outbreak of New Delhi metallo-beta-lactamase (NDM)-producing carbapenem-resistant *Klebsiella pneumoniae*, started in Tuscany, Italy, in November 2018 and continued in 2020 and through 2021. To understand the regional emergence and transmission dynamics over time, we collected and sequenced the genomes of 117 extensively drug-resistant, NDM-producing *K. pneumoniae* isolates cultured over a 20-month period from 76 patients at several health care facilities in South-East Tuscany. All isolates belonged to high-risk clone ST-147 and were typically non-susceptible to all first line antibiotics. Albeit sporadic, resistances to colistin, tigecycline and fosfomycin were also observed as a result of repeated, independent mutations. Genomic analysis revealed that ST-147 isolates circulating in Tuscany were monophyletic, highly genetically related (including a network of 42 patients from the same hospital and sharing nearly identical isolates) and shared a recent ancestor with clinical isolates from the Middle East. While the bla_{NDM-1} gene was carried by an IncFIB-type plasmid, our investigations revealed that the ST-147 lineage from Italy also acquired a hybrid IncH-type plasmid carrying the 16S methyltransferase *armA* gene as well as key virulence biomarkers often found in hypervirulent isolates. This plasmid shared extensive homologies with mosaic plasmids circulating globally including from ST-11 and ST-307 convergent lineages. Phenotypically, the carriage of this hybrid plasmid resulted in increased siderophore production but did not confer virulence to the level of an archetypical, hypervirulent *K. pneumoniae* in a subcutaneous model of infection with immunocompetent CD1 mice. Our findings highlight the importance of performing genomic surveillance to identify emerging threats.

52 **Significance Statement**

53 Carbapenem-resistant *Klebsiella pneumoniae* belong to the "critical priority" tier of bacterial

54 pathogens as identified by the World Health Organization. Emerging "high-risk" lineages are

55 responsible for difficult-to-treat, hospital-acquired infections and outbreaks around the globe. By

56 integrating genomic and epidemiological data for isolates collected over 20 months, this study

57 revealed both the high, regional prevalence and the rapid spread, within a single hospital, of *K.*

58 *pneumoniae* ST-147 in Italy. Besides resistance to nearly all antibiotics, we showed that this

59 lineage carried a hybrid plasmid harboring a set of biomarker genes previously linked to

60 hypervirulence. Convergence of multidrug resistance and hypervirulence is a major concern and

61 these findings highlight the need for robust, global surveillance to monitor the emergence of

62 high-risk *K. pneumoniae*.

Main Text

Introduction

63

64

65 *Klebsiella pneumoniae* is a leading cause of healthcare-associated infections including

66 pneumonia, urinary tract, and bloodstream infections (1). These classical *K. pneumoniae* (cKp)

67 frequently cause opportunistic infections in immunocompromised patients, elderly, neonates, and

68 patients with inserted medical devices (2). Of further concern, cKp strains can readily acquire

69 antimicrobial resistances including extended-spectrum betalactamases and carbapenemase-

70 encoding genes (3). Prompting a major public health challenge, the global emergence and

71 dissemination of multidrug resistant *K. pneumoniae* (MDR-cKp) is attributed to a few successful

72 clonal lineages, including newly identified "high-risk" sequence type (ST)-147 and ST-307 (4–

73 6). Similar to ST-307, the MDR-cKp ST-147 lineage emerged in Europe during the mid-1990s,

74 acquired plasmids encoding various carbapenemases genes (*i.e.*, VIM- and NDM-type metallo-β-

75 lactamases as well as OXA-48 serine-carbapenemase variants) in the mid-2000's, and has now

76 spread to all continents (4).

77 In recent years, a distinct hypervirulent pathotype (hvKp) has been identified, and is recognized

78 clinically by invasive and disseminated infections, in otherwise healthy individuals, that include

79 meningitis, liver abscesses, and endophthalmitis (2). However, the defining features of

80 hypervirulence remain ambiguous. Phenotypically, hvKp isolates have been characterized

81 primarily by their hypermucoviscosity, antimicrobial susceptibility, and greater production of

82 siderophores. Genetically, several virulence genes, carried on large virulence plasmids and

83 integrative conjugative elements (ICE), encoding for the biosynthesis of siderophores (aerobactin

84 [*iuc*], salmochelin [*iro*] and yersiniabactin [*ybt*]), the modulation of mucoviscosity and capsule

85   synthesis (*rmpADC/rmpA2),* metabolite transporter *peg-344,* and the production of genotoxic

86   polyketide colibactin (*clb*) have been linked to the hvKp pathotype (5, 7, 8)

87   Compounding the problem, convergent *K. pneumoniae* lineages with both virulence and

88   resistance genes have been observed, albeit infrequently (3, 9, 10). Genotypic convergence most

89   frequently occurs when MDR-cKp lineages acquire mobile genetic elements that carry the

90   aforementioned virulence biomarker genes (11). Alarmingly, large hybrid plasmids that harbor

91   both antimicrobial resistance and virulence genes have recently been reported in MDR isolates

92   from multiple countries (6, 12–16). This includes, sporadic instances of convergent *bla*$_{\text{NDM}}$-

93   carrying-ST-147 isolates detected in the United Kingdom (U.K.) in 2018 and 2019 (13, 14). Yet,

94   in most cases, the clinical impact and the resulting virulence potential of convergent lineages is

95   not well understood.

96   In this report, we investigated the emergence, genotypic convergence, phenotypic virulence, as

97   well as the regional and nosocomial spread of a NDM-producing ST-147 clone causing an

98   outbreak in Tuscany, Italy (17). This outbreak caused by an extensively drug-resistant (XDR) *K.*

99   *pneumoniae* was first identified in November 2018 in the Tuscany region where a significant

100 increase in reported cases from seven hospitals led to expanded surveillance practices (18, 19).

101 Recent surveillance data (Communicable Disease Threats Report 24-30 January 2021 by the

102 European Centre for Disease Prevention and Control) suggest that, at the time of writing, this

103 outbreak is ongoing with the risk of further transmission within and beyond Italy.

104 **Results**

105 **Emergence of the NDM-1 producing ST-147 outbreak clone in Italy.**

106 Between February 2019 and October 2020, a complete collection of NDM-producing *K.*

107 *pneumoniae* ST-147 from the University Teaching Hospital of Siena and several long-term

108 health care facilities in the South-East (SE) Tuscany region resulted in 117 isolates cultured from

109 76 patients (44% female; age ranging 27-96; median, 75) (**Table S1**). Similar to ST-147 strains

110 previously reported from the North-West (NW) region of Tuscany (19), these isolates were

111 predominantly non-susceptible to all tested penicillins, cephalosporins (including in combination

112 with a β-lactamase inhibitor), carbapenems, and aminoglycosides (**Table S2**). These 117 isolates

113 were mostly cultured from rectal swabs (74%; though the fraction of asymptomatic carriage is

114 unknown), urine (14%), respiratory tract (6%), or blood (5%) clinical samples. In 4/6 patients

115 (ID# 20, 25, 26, and 40) with bloodstream infections, positive rectal swab preceded blood

116 cultures suggesting gut-colonization resulted in invasive disease (**Table S1**). Whole-genome

117 sequencing (WGS) and phylogenetic analysis revealed that all ST-147 isolates from Italy

118 (including 9 publicly available genomes from bloodstream isolates collected in the NW Tuscany

119 (19)) were monophyletic (node 1) and showed high genetic relatedness (average pairwise

120 distance from nearest neighbor was 5.5 SNPs) (**Fig. 1**).

121 When compared to international ST-147 genomes (from both public databases and the MRSN

122 collection) the outbreak clone from Italy most closely resembled (shortest distance was 45 SNPs)

123 isolates collected from the Middle East (ME) between 2005 and 2015 (**Fig. 1 and S1**). All

124 isolates were predicted to be K-antigen capsular biosynthesis loci K64 and O-antigen type O2

125 variant 1 (O2v1) (**Table S1**). Further, the isolates from Italy carried a *bla*$_{NDM-1}$ metallo-β-

126 lactamase gene on an IncFIB-type plasmid (54,064 bp; hereby named pSI0739-NDM) (**Fig S2a**)

7

127   and a comparable plasmid (99% identity and 87% coverage) was found in 9 of 14 isolates from

128   the ME (**Fig 1**).

129

130   **Convergence of virulence and resistance genes.**

131   Genomic comparisons further identified that, since divergence from the ancestor shared with the

132   ME lineage, the ST-147 clone from Italy acquired a large hybrid IncH-type plasmid (335,489

133   bp), subsequently referred to as pSI0739-ARMA-Vir (**Fig S2b**). When compared to public

134   databases, pSI0739-ARMA-Vir was highly related to hybrid plasmids previously characterized

135   from various countries (U.K., Germany, and Czech Republic), and distinct convergent *K.*

136   *pneumoniae* lineages (ST-307, ST-15, ST-147, and ST-383) (**Table S3**) (6, 14, 20). In addition to

137   8 other antimicrobial resistance genes (**Fig. S2b**), pSI0739-ARMA-Vir carries the 16S rRNA

138   methyltransferase, *armA*, as well as virulence genes encoding a tellurium resistance operon

139   (*terZABCDEF*), aerobactin biosynthesis (*iuc1*), putative hypermucoidy and capsule synthesis

140   loci (*rmpADC/rmpA2*), and the metabolite transporter, *peg-344* (**Fig. 1 and S2b**). 92% of isolates

141   also carry genes encoding the yersiniabactin siderophore system (*ybt9* lineage harbored by a

142   chromosomal ICEKp3).

143   Within the outbreak isolates from Tuscany, the presence or absence of plasmid-bound resistance

144   and virulence genes was used to identify excision events or plasmid loss (labelled A-K) (**Fig. 1**

145   **and S2b**). In four independent instances (A, B, I, and J) a ~ 60 to 90 Kb segment containing the

146   virulence genes was excised from pSI0739-ARMA-Vir (**Fig. 1 and S2b**). Insertion sequences

147   (IS) were often identified at the boundaries of the virulence island, suggesting transposition

148   could play a role in the mosaic structure of these plasmids, as previously proposed (14). Notably,

149   excision event B occurred within the host where (2 out of 5) serial isolates from patient 19

150   eventually lost all virulence genes (**Fig. 1 and S2b**). The *armA* gene cassette, flanked by IS*26*

151   elements, was also excised on three separate occasions (D, E and F; the latter as the likely result

152   of in-host evolution within serial isolates from patient 4). By contrast, the complete pSI0739-

153   ARMA-Vir was lost in three of the later isolates (July and August 2020; event K); all highly

154   genetically related but from distinct patients (**Fig. 1 and S2b**). Plasmid loss was also observed

155   for pSI0739-NDM (three distinct events D, G, and H) (**Fig. S2b**). As expected, susceptibility to

156   the aminoglycosides and/or carbapenems was restored in these isolates (**Table S2**).

157

158   **ST-147 outbreak is fueled by nosocomial spread.**

159   Phylogenetic analysis of the isolates from Tuscany revealed the existence of two clades

160   (differing by 32.9 SNPs on average), A and B (**Fig. 1**). Clade A was relatively heterogenous

161   (average pairwise distance from nearest neighbor was 11.1 SNPs) and comprised 31 isolates

162   from 23 patients at 3 distinct healthcare facilities in SE Tuscany (**Fig. 1 and Table S1)**.

163   Additionally, clade A includes 9 genomes from a hospital in NW Tuscany for which patient

164   metadata is unknown (19). In contrast, clade B was highly homogeneous (average distance of 2.4

165   SNPs from nearest neighbor) and grouped 86 isolates collected from 57 inpatients from the Siena

166   University Teaching hospital.

167   Temporally, detection of the first clade A isolate from each patient (*i.e.* removing serial isolates)

168   was relatively stable (1.2 new cases per month on average) across the 20-month sampling period

169   (**Fig. 2a**). By contrast, a large increase of new cases due to clade B isolates (7.1 cases per month)

170   was observed over a 6-month period (July to December 2019). Further, the majority (90%) of

171   clade B isolates were collected from only 5 wards with few patients (n = 10) yielding positive,

172   serial cultures from multiple wards **(Fig. 2b)**. To trace possible nosocomial events, patient pairs

9

173 that shared an isolate separated by 4 SNPs or less were identified and used to construct a network

174 of possible transmission. This approach ultimately linked 74% (n = 42) of all patients

175 represented in clade B and revealed that 8 inpatients (ID# 7, 9, 10, 14, 18, 20, 22, and 23), all in

176 the cardiology clinic in July and August of 2019, shared genetically identical isolates (**Fig. 2bc**).

177 While the last case detected in the cardiology clinic was in September 2019, this clone had

178 seemingly spread throughout the hospital. Indeed, between September 2019 and October 2020,

179 the internal medicine and emergency wards accounted for 75% of primary cases due to a clade B

180 isolate (**Fig. 2bc**). Of note, the apparent reduction in isolates collected from patients between

181 February and July 2020 was likely the result of hospital policies to reduce the number of non-

182 urgent programmed hospitalizations in relation to the COVID-19 pandemic. New cases (*e.g.*

183 patients 69-72) quickly reappeared in the fall of 2020 indicating nosocomial transmission of

184 clade B was not yet contained (**Fig. 2ab**).

185

186 **Positive selection on resistance and virulence determinants.**

187 In addition to some isolates independently excising regions within or the whole pSI0739-

188 ARMA-Vir and pSI0739-NDM plasmids, mutational convergence was also observed within

189 specific genes and functional clusters. The most striking example was gene *glpT* that encodes the

190 main transporter responsible for the uptake of the fosfomycin antibiotic. Not accounting for

191 synonymous (SYN) mutations, 10 variants emerged independently in *glpT* (4 predicted loss-of-

192 function [LOF] and 6 non-synonymous [NSY] mutations) and were found in 24 outbreak

193 isolates, mostly from clade A (**Fig. 3**). This is in agreement with a previous report of *glpT*

194 mutations found in clinical, epidemic ST-147 isolates that was likely responsible for reduced

195 fosfomycin susceptibility (21). Four distinct NSY mutations in the *cusSRA* cluster, previously

196   associated with copper and silver, and tigecycline resistance (22), were found in 6 isolates from

197   both clades (**Fig. 3**). In addition, the *ramR-ramA* gene cluster, consisting of the *romA-ramA*

198   operon and the divergently transcribed *ramR* (resistance antibiotic multiple protein A), was

199   mutated at 7 distinct occurrences (including 2 predicted LOF in *ramR* and one in *romA*) in 20

200   strains (**Fig. 3**). Two serial isolates from patient 4 with the same frameshift mutation in *ramR*

201   demonstrated tigecycline resistance (MIC ≥ 8 mg/L), consistent with previous reports in *K.*

202   *pneumoniae* (23) (**Fig. S4b and Table S2**). Notably, isolate 752623 also evolved tigecycline

203   resistance, but the genetic determinants remain unclear (**Table S2**). The other predicted LOF

204   mutations in both *ramR* and *romA* were found in 5 genetically related isolates from NW Tuscany

205   (Kp-P1, Kp-P2, Kp-11Pi, Kp-12Pi and Kp-16Pi) for which decreased susceptibility to

206   tigecycline was noted (19). Interestingly, Falcone *et al*. also reported that: i) isolates Kp-P1 and

207   Kp-P2 carried *bla*NDM−9, which differs from *bla*NDM−1 by a single amino acid substitution and

208   confers higher levels of resistance to the carbapenems, and ii) isolates Kp-P1, Kp-P2, Kp-12Pi,

209   and Kp-16Pi evolved resistance to colistin in part due to loss of function mutations in *mgrB* (19).

210   Here, isolate 849820 carried a truncated *mgrB* (**Table S1**) but remained susceptible to colistin

211   (MIC < 0.25 mg/L). Positive selection was also observed for genes involved in cell wall

212   synthesis (*pbp2*, *pbp3*, *rlpA*) and glycosylation (*pglA*), adhesion to mucosal surfaces and

213   virulence (*fimH*), nitrate respiration (*narLXG*), and iron binding and transport (*sufBDS*) (**Fig. 3**).

214   The latter was recently reported as a potential factor underlying the persistence of an outbreak

215   involving high-risk ST-258 *K. pneumoniae* (24).

216

217   **Fixation of variants through patient transmission and within host evolution.**

218   To further identify traits that possibly contributed to the success and spread of the ST-147 clone

219   in hospitals in Tuscany, we identified variants that became fixed in the population at nodes of

220   interest (excluding SYN and intergenic variants) (**Fig. S3a**). Using parsimony, we identified 8

221   variants found in all isolates from Italy that were missing in all ME genomes (node 1). Of

222   particular interest were: (i) a predicted LOF mutation in *cycA* which encodes a Serine/Alanine

223   transporter that, when functional, allows the antibiotic D-cycloserine to cross the cell wall and

224   reach its cytoplasmic target (25), (ii) a NSY mutation in *pabA* involved in aromatic amino acid

225   biosynthesis and previously characterized as a general infection requirement for *K. pneumoniae*

226   (26), and (iii) a NSY mutation in *hdfR* encoding for a transcriptional regulator involved in the

227   complex regulation of capsule production and hypermucoviscosity (27).

228   Two NSY variants (in genes *fliY* and *ybiO*) arose in the last common ancestor at the root of clade

229   A (node 2) while a total of 9 variants arose at the root (nodes 3 and 4) of clade B (**Fig. 1 and**

230   **S3a**). Among them, variants in two genes could participate in the apparent success of clade B in

231   spreading and persisting in the hospital: *metQ* a D-methionine-binding lipoprotein, shown to be

232   important for colonization (28), and *pal*, encoding a peptidoglycan-associated lipoprotein shown

233   to provide protection against neutrophil phagocytosis and killing as well resistance to

234   gastrointestinal bile salts (29), a key ability for transmission via the fecal-oral route.

235   Similarly, longitudinal sampling of six serial isolates (March 2019 to January 2020) from patient

236   4 revealed a stepwise, fixation of variants (**Fig. S3b**). NSY mutations were present in genes

237   involved in cell wall biosynthesis/recycling (*rlpA*, *emtA*) and surface polysaccharide synthesis

238   (*rffG*). The latter is part of a gene cluster that encodes the Enterobacterial Common Antigen

239   (ECA), a carbohydrate polymer thought to play a significant role in *K. pneumoniae* physiology

240   and host interactions (26). Amino acid substitutions in the adhesin *fimH* and in the

241   multifunctional regulator *mgrA*, were also observed in these serial isolates.

242

243   **Pathogenicity of the convergent ST-147 clone from Italy.**

244   While sequencing allowed for the detection of genotypic convergence, the virulence of this

245   epidemic ST-147 clone remained to be established. Two distinct outbreak isolates carrying

246   pSI0739-ARMA-Vir (752019 and 752165) produced siderophore at levels well above the 30 µg/ml

247   threshold predictive of the hvKp pathotype (~230 µg/ml; **Fig. 4a and S4a**) (30). The excision of

248   virulence genes (including the *iuc* siderophore biosynthesis operon) in outbreak isolate 752253

249   (event B, **Fig. S2b**) resulted in siderophore levels comparable to the cKP1 control (**Fig. S4a**).

250   However, despite carrying the virulence genes *rmpADC* and *rmpA2*, isolates 752019 and 752165

251   showed mucoviscosity levels comparable to the cKP1 control (**Fig. 4b and S4b**). Moreover, a

252   subcutaneous (SQ) model of infection with immunocompetent CD1 mice determined that 752019

253   and 752165 were non-lethal at a challenge inoculum of 10^3 CFU, unlike canonical hypervirulent

254   isolate hvKP2 (**Fig. 4c**). Further, no lethality was observed with a 10^5 CFU inoculum of the ST-

255   147 isolates and only SQ challenges with 10^7 and 10^8 CFU revealed a slight increase in lethality

256   (non-significant for 752019 [**Fig. 4c**]; p=0.029 for 752165 at 10^8 CFU [**Fig. S5**]) when compared

257   to the cKP1 control, which was consistently found as non-lethal at a challenge inoculum up to 2.5

258   x 10^8 CFU (31). Likewise, SQ challenge with strain PBIO1953 (6), a convergent ST-307 *K.*

259   *pneumoniae* outbreak clone carrying a hybrid plasmid with extensive similarity pSI0739-ARMA-

260   Vir (**Table S3**), resulted in mortality rate of 20% at the highest inoculum (not reaching statistical

261   significance) compared to the cKP1 control (**Fig. S5**).

262

13

Discussion

We report a comprehensive analysis of an NDM-producing ST-147 *K. pneumoniae* outbreak

clone circulating in Tuscany, Italy. Although the number of colonized/infected patients was

significantly lower than in the North-West region (18), our study demonstrates that this

epidemic, XDR clone has now spread throughout multiple healthcare facilities in the South-East

region of Tuscany. Phylogenetic analysis suggests that this clone possibly emerged from a

NDM-1-producing, ST-147, MDR-cKp lineage, previously shown to be endemic in the Middle

East (32), by acquiring a hybrid resistance/virulence plasmid. Furthermore, we also confirm the

early concern about cross-border spread (17), as highly genetically related isolates (**Fig. S1**),

with near identical plasmids (**Table S3**), have been reported in multiple U.K. hospitals in 2018

and 2019 (14).

Signs of strong selective pressure was observed in genes associated with drug resistance. With

the prototypical ST-147 outbreak isolate resisting to all first line agents (*i.e.* beta-lactams,

including carbapenems; fluoroquinolones; aminoglycosides) (**Table S2**), effective treatment

relies on second line antibiotics (*e.g.* colistin, tigecycline and fosfomycin) as well as combination

therapies (33). In this context, the repeated, independent emergence of variants associated with

resistance to either fosfomycin (*glpT*), tigecycline (*ramR*), and colistin (*mgrB*) is particularly

worrisome and raises the concern of the emergence of a pan-resistant ST-147 epidemic lineage.

While WGS allows for the detection of convergence events in *K. pneumoniae*, the definitive

impact on pathogenicity often remains unclear (3, 31). Compared to this ST-147 clone from

Italy, the acquisition of the same combination of virulence genes was reported in distinct

lineages of *K. pneumoniae* ST-11 from China and Egypt (15, 16), and ST-307 from Germany

(6). Comparable virulence was observed in a *Galleria* insect model at 10^6 CFU of ST-11 strains

14

286   with and without the virulence plasmid (15). Furthermore, using clinical cohort stratifying, no

287   increased mortality was observed in patients infected with ST-11 isolates, carrying the virulence

288   plasmid, (15). The recent ST-307 epidemic clone from Germany carried a near identical hybrid

289   plasmid to pSI0739-ARMA-Vir (**Table S3**) and similarly showed increased siderophore

290   production directly tied to the presence of the virulence genes (6). Here, a SQ challenge of

291   immunocompetent CD1 mice unequivocally demonstrates that isolates from both lineages (ST-

292   147 from Italy and ST-307 from Germany) did not exhibit a maximal hypervirulent phenotype

293   (where lethality is observed with $< 10^3$ CFU (31)) and were only slightly more lethal than a cKP,

294   at the highest inoculum tested. Nonetheless, a small increase in pathogenic potential may be

295   clinically significant, particularly in the healthcare setting in which patients are variably

296   immunocompromised.

297   Based on the current knowledge of *K. pneumoniae* pathogenicity, the reason(s) for the minimal

298   virulence of the convergent ST-147 and ST-307 outbreak clones remains unclear. While

299   increased siderophore production was historically associated with hvKp isolates (34, 35), we

300   have recently shown that this measurement only partially correlates with virulence differences *in*

301   *vivo* (31). The same observation was made for hypermucoviscosity (31), which, despite the

302   presence of the required *rmpADC*/*rmpA2* genes, was not observed in this ST-147 clone. Other

303   possible reasons are the absence of other known virulence factors (*e.g.* salmochelin and

304   colibactin), genes whose role in virulence has yet to be recognized, virulence gene

305   polymorphism, and differences in capsule type. In this latter possibility, ST-147 isolates are K-

306   antigen type 64, unlike the highly serum resistant K1 and K2 capsules often associated with

307   hvKp isolates (3). Finally, tight regulation of virulence determinants could mitigate the potential

308   biological cost of expressing the many genes on these large hybrid plasmids, a barrier previously

309   proposed as a reason for the relative rarity of convergent strains (3).

310   The role played by this IncH hybrid plasmid, and the selective forces underlying its emergence in

311   distinct MDR *K. pneumoniae* lineages, remains a central question. While the presence of

312   antibiotic resistance genes undoubtedly confers a selective advantage (36), a hypothesis would

313   be that acquisition of other genes carried by this IncH hybrid plasmid confer increased

314   colonization or persistence abilities, traits not examined in our systemic infection model. This

315   could bear clinical significance as high loads of *K. pneumoniae* in the GI tract have been

316   associated with elevated risk of bacteremia (37). In our collection, most ST-147 isolates were

317   recovered from rectal swabs. Previous work did demonstrate that MDR-cKp colonized poorly in

318   comparison to hvKP1, suggesting an advantage might exist for carrying the virulence plasmid in

319   the gut (38). In fact, increased siderophore production, the one feature observed in ST-147 and a

320   direct result of the presence of the hybrid plasmid, has already been proposed to facilitate gut

321   colonization and spread of various pathogenic *Enterobacterales* (39, 40). Finally, a tellurium

322   resistance operon (*terZABCDEF*), harbored by the IncH hybrid plasmid in both ST-147 and ST-

323   307 outbreak clones, has recently been proposed as a microbiome-dependent fitness factor

324   involved in gut colonization in a murine model (41).

325   In summary, we identified a convergent clone of ST-147 that shares a recent common ancestor

326   with isolates collected in the Middle East and has been sporadically detected in multiple

327   hospitals in the U.K.. While this outbreak clone was XDR, the maximal hypervirulent phenotype

328   was not observed in immunocompetent hosts *in vivo* despite the presence of a hybrid

329   resistance/virulence plasmid. Further studies are needed to fully characterize the role of these

330   plasmids and the drivers of their emergence in distinct lineages of MDR-Kp around the globe.

16

331   Close monitoring of global *K. pneumoniae* populations, as well as ongoing, local efforts to

332   contain the dissemination of such high-risk clones are critical to impede the emergence of this

333   troublesome pathogen.

334

Materials and Methods

Bacterial Isolates and Antibiotic Susceptibility Testing. The complete set of XDR *K.*

pneumoniae isolates (**Table S1**) were collected from the University Teaching Hospital of Siena

(Azienda Ospedaliera Universitaria Senese AOUS), Italy, a 700-bed regional health care facility

providing microbiological analyses in the frame of a regional surveillance network for several

other local healthcare facilities part of the South-East district and long-term healthcare structures.

Bacterial identification and antimicrobial susceptibility testing were carried out using the

MALDI Biotyper (Bruker Daltonics GmbH, Bremen, Germany) and the Becton Dickinson

Phoenix M50 (Eysins, Switzerland). Carbapenemase production was confirmed using the

mSuperCARBA medium (ChromAgar, Paris, France). β-lactamase genes were identified using a

PCR analysis (Cica Geneus ESBL Genotype Detection kit, Cica Geneus AmpC Genotype

Detection kit and Cica Geneus Carbapenemase Genotype Detection kit 2, Kanto Chemical Co.,

Tokyo, Japan), as recommended by the manufacturer. Isolates were sent to the Multidrug

Resistant Organism Repository and Surveillance Network (MRSN) for further phenotypic

characterization and genome sequencing. Confirmatory antibiotic susceptibility testing (AST)

was performed in the MRSN College of American Pathologists (CAP)-accredited clinical lab

using the Vitek 2 (card GN AST 71 and GN ID; bioMérieux, NC, USA) (**Table S2**). MICs of

colistin were determined in triplicate using the broth microdilution method following Clinical

and Laboratory Standards Institute guidelines.

Whole Genome Sequencing. Genomic DNA was extracted and sequenced via Illumina MiSeq

or NextSeq benchtop sequencer (Illumina, Inc., San Diego, CA) as previously described (42).

For isolate 752165 (alternate name SI-0739) long read sequencing was carried out using a

MinION sequencer (Oxford Nanopore Technologies). Basecalling was performed using Guppy

359   (configuration r9.4.1_450bps_hac), filtered using Filtlong (https://github.com/rrwick/Filtlong)

360   and hybrid assembly was performed using Unicycler (43). Complete plasmids, pSI0739-ARMA-

361   Vir and pSI0739-NDM, from isolate SI-0739 were used as reference for plasmid comparison. All

362   genomes have been deposited in the National Center for Biotechnology Information under

363   BioProject PRJNA725484.

364   **Bioinformatic analysis.** Species identification, MLST typing, virulence locus, capsule (K), and

365   lipopolysaccharide (O) loci were identified using Kleborate v2.0.1 (**Table S1**) (44). The *peg-344*

366   gene was identified using BLASTn search of draft genome assemblies (query sequence pLVPK,

367   accession number NC_005249). AMRFinderPlus v3.9.8 (45) and ARIBA v2.14.4 (46) were used

368   to identify resistance alleles from draft assemblies and processed reads, respectively, followed by

369   deduplication of redundant alleles calls. cgMLST allele assignment and minimum spanning tree

370   generation were performed with SeqSphere (47).

371   We created a SNP phylogeny for ST-147 including the 117 outbreak isolates, 9 previously

372   published genomes (19), and 14 MRSN genomes from ME and Germany (**Table S1**). SNP

373   calling was performed with Snippy v.4.4.5 (https://github.com/tseemann/snippy) using error

374   corrected [Pilon v1.23 (48)] and annotated [Prokka v1.14.6 (49)] draft assembly of 752019 as the

375   reference (**Table S4**). The core SNP alignment was filtered for recombination using Gubbins

376   v2.4.1 (50), which identified 587 variant sites. A maximum likelihood tree was inferred with

377   RAxML-NG v1.0.1 (51) using GTR+G (50 parsimony, 50 random) and was midpoint rooted in

378   iTOL v. 5.5 (52) for visualization with metadata.

379   For the patient transmission network, a pairwise SNP matrix for clade B isolates was obtained

380   using Snippy v.4.4.5 and snp-dist v.0.7.0 (https://github.com/treemann/snp-dists). Distances ≤ 4

381   SNPs between isolates from distinct patients were identified. In cases of serial isolates with

382   varying distances, only the lowest inter-patient SNP distance was retained. The resulting network

383   of patients was visualized and edited using Flourish (https://flourish.studio/).

384   Plasmid content comparisons were performed using closed plasmids pSI0739-NDM and

385   pSI0739-ARMA-Vir as a reference. The draft genomes of outbreak isolates were mapped against

386   the closed reference plasmids using default parameters of the CGView server (http://cgview.ca/).

387   **Mucoviscosity and quantitative siderophore assays.**

388   Mucoviscosity of selected isolates was measured (ratio of OD_{600} values post/pre centrifugation at

389   1,000 x g for 5 minutes) after 24 hours of growth (37°C and 275 rpm) in LB or c-M9-te minimal

390   medium (M9), as described previously (31).

391   To quantify siderophore production, the isolates of interest were grown overnight at 37°C in

392   iron-chelated M9 minimal media containing casamino acids (c-M9-CA) and culture supernatants

393   were assessed using the chromeazurol S dye assay as described (35). For both *in vitro* essays,

394   three independent biological replicates were performed on different days for each strain and the

395   data was reported as the mean ± the SD.

396   **Mouse subcutaneous (SQ) infection model.**

397   Animal studies were reviewed and approved by the Veterans Administration Institutional Animal

398   Care Committee and the University at Buffalo-SUNY and were carried out in strict accordance

399   with the recommendations in the guidelines delineated in the "NIH Guide for the Care and Use

400   of Laboratory Animals"(revised 1985) and the "Ethics of Animal Experimentation Statement"

401   (Canadian Council on Animal Care, July, 1980) as monitored by the Institutional Animal Care

402   and Use Committee. All efforts were made to minimize suffering. Veterinary care for the

403   animals was supplied by the staff of Veterans Administration Animal Facility under the direction

404   of a fully licensed veterinarian. CD1 male mice, 4-6 weeks old, were obtained from Charles

405   River Laboratories, quarantined for 5 days before use, and challenged via a SQ injection with the

406   isolates of interest (100 μL of bacterial suspension serially diluted to the required titers in 1 x

407   PBS diluted and injected using a 0.5 mL insulin syringe), as previously described (31). The

408   animals were closely monitored for 14 days after challenge for the development of the study

409   endpoints, survival or severe illness (in extremis state)/death, which was recorded as a

410   dichotomous variable. Signs that were monitored and which resulted in immediate euthanasia

411   using methods consistent with the recommendations of the American Veterinary Medical

412   Association Guidelines included hunched posture, ruffled fur, labored breathing, reluctance to

413   move, photophobia, and dehydration

414   **Statistical analyses.**

415   Statistical analyses were performed using GraphPad Prism 8.0. A Log-rank (Mantel-Cox) test

416   was performed to analyze *in vivo* infection model data. A Mann-Whitney test was used to

417   compare siderophore concentrations between strains. Bonferroni posttests were used to account

418   for multiple comparisons. A *P* value < 0.05 was considered statistically significant.

References

1. R. Podschun, U. Ullmann, Klebsiella spp. as Nosocomial Pathogens: Epidemiology, Taxonomy, Typing Methods, and Pathogenicity Factors. *Clin. Microbiol. Rev.* **11**, 589–603 (1998).

2. T. A. Russo, C. M. Marr, Hypervirulent *Klebsiella pneumoniae*. *Clinical Microbiology Reviews* **32**, 42 (2019).

3. S. Gonzalez-Ferrer, *et al.*, Finding Order in the Chaos: Outstanding Questions in *Klebsiella pneumoniae* Pathogenesis. *Infect Immun* **89**, e00693-20, /iai/89/4/IAI.00693-20.atom (2021).

4. G. Peirano, L. Chen, B. N. Kreiswirth, J. D. D. Pitout, Emerging Antimicrobial-Resistant High-Risk *Klebsiella pneumoniae* Clones ST307 and ST147. *Antimicrob Agents Chemother* **64**, e01148-20, /aac/64/10/AAC.01148-20.atom (2020).

5. K. L. Wyres, M. M. C. Lam, K. E. Holt, Population genomics of *Klebsiella pneumoniae*. *Nat Rev Microbiol* **18**, 344–359 (2020).

6. S. E. Heiden, *et al.*, A *Klebsiella pneumoniae* ST307 outbreak clone from Germany demonstrates features of extensive drug resistance, hypermucoviscosity, and enhanced iron acquisition. *Genome Med* **12**, 113 (2020).

7. K. A. Walker, L. P. Treat, V. E. Sepúlveda, V. L. Miller, The Small Protein RmpD Drives Hypermucoviscosity in. **11**, 14 (2020).

8. J. Bulger, U. MacDonald, R. Olson, J. Beanan, T. A. Russo, Metabolite Transporter PEG344 Is Required for Full Virulence of Hypervirulent *Klebsiella pneumoniae* Strain hvKP1 after Pulmonary but Not Subcutaneous Challenge. *Infect Immun* **85**, e00093-17, e00093-17 (2017).

9. D. Gu, *et al.*, A fatal outbreak of ST11 carbapenem-resistant hypervirulent *Klebsiella pneumoniae* in a Chinese hospital: a molecular epidemiological study. *The Lancet Infectious Diseases* **18**, 37–46 (2018).

10. K. L. Wyres, *et al.*, Genomic surveillance for hypervirulence and multi-drug resistance in invasive *Klebsiella pneumoniae* from South and Southeast Asia. *Genome Med* **12**, 11 (2020).

11. K. L. Wyres, *et al.*, Distinct evolutionary dynamics of horizontal gene transfer in drug resistant and virulent clones of *Klebsiella pneumoniae*. *PLoS Genet* **15**, e1008114 (2019).

12. M. M. C. Lam, *et al.*, "Genomic surveillance framework and global population structure for *Klebsiella pneumoniae*" (Genomics, 2020) https:/doi.org/10.1101/2020.12.14.422303 (April 1, 2021).

13. J. F. Turton, *et al.*, Virulence genes in isolates of *Klebsiella pneumoniae* from the UK during 2016, including among carbapenemase gene-positive hypervirulent K1-ST23 and 'non-hypervirulent' types ST147, ST15 and ST383. *Journal of Medical Microbiology* **67**, 118–128 (2018).

14. J. Turton, *et al.*, Hybrid Resistance and Virulence Plasmids in "High-Risk" Clones of *Klebsiella pneumoniae*, Including Those Carrying blaNDM-5. *Microorganisms* **7**, 326 (2019).

15. K. Zhou, *et al.*, Novel Subclone of Carbapenem-Resistant *Klebsiella pneumoniae* Sequence Type 11 with Enhanced Virulence and Transmissibility, China. *Emerg. Infect. Dis.* **26**, 289–297 (2020).

468 16. M. A. E.-G. E.-S. Ahmed, *et al.*, Emergence of Hypervirulent Carbapenem-Resistant *Klebsiella*
469   *pneumoniae* Coharboring a *bla* NDM-1 -Carrying Virulent Plasmid and a *bla* KPC-2 -Carrying Plasmid
470   in an Egyptian Hospital. *mSphere* **6**, e00088-21 (2021).

471 17. European Centre for Disease Prevention and Control, Regional outbreak of New Delhi metallo-
472   beta-lactamase-producing carbapenem-resistant Enterobacteriaceae, Italy, 2018–2019. 7 (2018).

473 18. L. Tavoschi, *et al.*, Prolonged outbreak of New Delhi metallo-beta-lactamase-producing
474   carbapenem-resistant Enterobacterales (NDM-CRE), Tuscany, Italy, 2018 to 2019.
475   *Eurosurveillance* **25**, 7 (2020).

476 19. M. Falcone, *et al.*, Extremely drug-resistant NDM-9-producing ST147 *Klebsiella pneumoniae*
477   causing infections in Italy, May 2020. *Eurosurveillance* **25**, 6 (2020).

478 20. K. Chudejova, *et al.*, Genetic Plurality of OXA/NDM-Encoding Features Characterized From
479   Enterobacterales Recovered From Czech Hospitals. *Front. Microbiol.* **12**, 641415 (2021).

480 21. K. Avgoulea, *et al.*, Characterization of Extensively Drug-Resistant or Pandrug-Resistant
481   Sequence Type 147 and 101 OXA-48-Producing *Klebsiella pneumoniae* Causing Bloodstream
482   Infections in Patients in an Intensive Care Unit. *Antimicrob Agents Chemother* **62**, e02457-17
483   (2018).

484 22. D. Chen, *et al.*, CusS-CusR Two-Component System Mediates Tigecycline Resistance in
485   Carbapenem-Resistant *Klebsiella pneumoniae*. *Front. Microbiol.* **10**, 3159 (2020).

486 23. Y. Mao, Q. Shi, P. Zhang, Y. Jiang, Y. Yu, Effect of ramR loss-of-function insertion on
487   tigecycline resistance in clinical isolates of carbapenem-resistant *Klebsiella pneumoniae*. *Journal*
488   *of Global Antimicrobial Resistance* **21**, 410–413 (2020).

489 24. J. W. Marsh, *et al.*, Evolution of Outbreak-Causing Carbapenem-Resistant *Klebsiella pneumoniae*
490   ST258 at a Tertiary Care Hospital over 8 Years. *mBio* **10**, e01945-19 (2019).

491 25. V. Dengler, P. Meier, R. Heusser, B. Berger-Bachi, N. McCallum, Induction kinetics of the
492   *Staphylococcus aureus* cell wall stress stimulon in response to different cell wall active antibiotics.
493   *BMC Microbiology* **11**, 16 (2011).

494 26. S. Bruchmann, T. Feltwell, J. Parkhill, F. L. Short, Identifying virulence determinants of
495   multidrug-resistant *Klebsiella pneumoniae* in Galleria mellonella. *Pathogens and Disease* **79**
496   (2021).

497 27. L. A. Mike, *et al.*, A systematic analysis of hypermucoviscosity and capsule reveals distinct and
498   overlapping genes that impact Klebsiella pneumoniae fitness. *PLoS Pathog* **17**, e1009376 (2021).

499 28. S. Basavanna, *et al.*, The Effects of Methionine Acquisition and Synthesis on *Streptococcus*
500   *Pneumoniae* Growth and Virulence. *PLoS ONE* **8**, e49638 (2013).

501 29. P.-F. Hsieh, *et al.*, *Klebsiella pneumoniae* Peptidoglycan-Associated Lipoprotein and Murein
502   Lipoprotein Contribute to Serum Resistance, Antiphagocytosis, and Proinflammatory Cytokine
503   Stimulation. *Journal of Infectious Diseases* **208**, 1580–1589 (2013).

504   30.   T. A. Russo, *et al.*, Identification of Biomarkers for Differentiation of Hypervirulent *Klebsiella*
505   *pneumoniae* from Classical *K. pneumoniae*. *J Clin Microbiol* **56**, e00776-18 (2018).

506   31.   T. A. Russo, *et al.*, An Assessment of Siderophore Production, Mucoviscosity, and Mouse
507   Infection Models for Defining the Virulence Spectrum of Hypervirulent *Klebsiella pneumoniae*.
508   *mSphere* **6**, e00045-21 (2021).

509   32.   K. Xanthopoulou, *et al.*, Antibiotic Resistance and Mobile Genetic Elements in Extensively Drug-
510   Resistant *Klebsiella pneumoniae* Sequence Type 147 Recovered from Germany. *Antibiotics* **9**, 675
511   (2020).

512   33.   N. Petrosillo, M. Giannella, R. Lewis, P. Viale, Treatment of carbapenem-resistant *Klebsiella*
513   *pneumoniae* : the state of the art. *Expert Review of Anti-infective Therapy* **11**, 159–177 (2013).

514   34.   T. A. Russo, R. Olson, U. MacDonald, J. Beanan, B. A. Davidson, Aerobactin, but Not
515   Yersiniabactin, Salmochelin, or Enterobactin, Enables the Growth/Survival of Hypervirulent
516   (Hypermucoviscous) *Klebsiella pneumoniae* Ex Vivo and In Vivo. *Infection and Immunity* **83**, 9
517   (2015).

518   35.   T. A. Russo, *et al.*, Aerobactin Mediates Virulence and Accounts for Increased Siderophore
519   Production under Iron-Limiting Conditions by Hypervirulent (Hypermucoviscous) *Klebsiella*
520   *pneumoniae*. *Infection and Immunity* **82**, 2356–2367 (2014).

521   36.   E. Gullberg, L. M. Albrecht, C. Karlsson, L. Sandegren, D. I. Andersson, Selection of a Multidrug
522   Resistance Plasmid by Sublethal Levels of Antibiotics and Heavy Metals. *mBio* **5**, e01918-14
523   (2014).

524   37.   T. Shimasaki, *et al.*, Increased Relative Abundance of *Klebsiella pneumoniae* Carbapenemase-
525   producing *Klebsiella pneumoniae* Within the Gut Microbiota Is Associated With Risk of
526   Bloodstream Infection in Long-term Acute Care Hospital Patients. *Clinical Infectious Diseases* **68**,
527   2053–2059 (2019).

528   38.   T. M. Young, *et al.*, Animal Model To Study *Klebsiella pneumoniae* Gastrointestinal Colonization
529   and Host-to-Host Transmission. *Infect Immun* **88**, e00071-20 (2020).

530   39.   J. Behnsen, *et al.*, The Cytokine IL-22 Promotes Pathogen Colonization by Suppressing Related
531   Commensal Bacteria. *Immunity* **40**, 262–273 (2014).

532   40.   L. J. Searle, G. Méric, I. Porcelli, S. K. Sheppard, S. Lucchini, Variation in Siderophore
533   Biosynthetic Gene Distribution and Production across Environmental and Faecal Populations of
534   *Escherichia coli*. *PLoS ONE* **10**, e0117906 (2015).

535   41.   J. Vornhagen, *et al.*, A plasmid locus associated with *Klebsiella* clinical infections encodes a
536   microbiome-dependent gut fitness factor. *PLoS Pathog* **17**, e1009537 (2021).

537   42.   M. R. Galac, *et al.*, A Diverse Panel of Clinical *Acinetobacter baumannii* for Research and
538   Development. *Antimicrob Agents Chemother* **64**, e00840-20 (2020).

539   43.   R. R. Wick, L. M. Judd, C. L. Gorrie, K. E. Holt, Unicycler: Resolving bacterial genome
540   assemblies from short and long sequencing reads. *PLoS Comput Biol* **13**, e1005595 (2017).

541   44.   M. M. C. Lam, R. R. Wick, K. L. Wyres, K. E. Holt, Genomic surveillance framework and global
542   population structure for *Klebsiella pneumoniae*. bioRxiv
543   https:/doi.org/10.1101/2020.12.14.422303 (February 2, 2021).

544   45.   M. Feldgarden, *et al.*, Validating the AMRFinder Tool and Resistance Gene Database by Using
545   Antimicrobial Resistance Genotype-Phenotype Correlations in a Collection of Isolates. *Antimicrob*
546   *Agents Chemother* **63**, e00483-19 (2019).

547   46.   M. Hunt, *et al.*, ARIBA: rapid antimicrobial resistance genotyping directly from sequencing reads.
548   *Microbial Genomics* **3** (2017).

549   47.   S. Jünemann, *et al.*, Updating benchtop sequencing performance comparison. *Nat Biotechnol* **31**,
550   294–296 (2013).

551   48.   B. J. Walker, *et al.*, Pilon: An Integrated Tool for Comprehensive Microbial Variant Detection and
552   Genome Assembly Improvement. *PLoS ONE* **9**, e112963 (2014).

553   49.   T. Seemann, Prokka: rapid prokaryotic genome annotation. *Bioinformatics* **30**, 2068–2069 (2014).

554   50.   N. J. Croucher, *et al.*, Rapid phylogenetic analysis of large samples of recombinant bacterial whole
555   genome sequences using Gubbins. *Nucleic Acids Research* **43**, e15–e15 (2015).

556   51.   A. M. Kozlov, D. Darriba, T. Flouri, B. Morel, A. Stamatakis, RAxML-NG: a fast, scalable and
557   user-friendly tool for maximum likelihood phylogenetic inference. *Bioinformatics* **35**, 4453–4455
558   (2019).

559   52.   I. Letunic, P. Bork, Interactive Tree Of Life (iTOL) v4: recent updates and new developments.
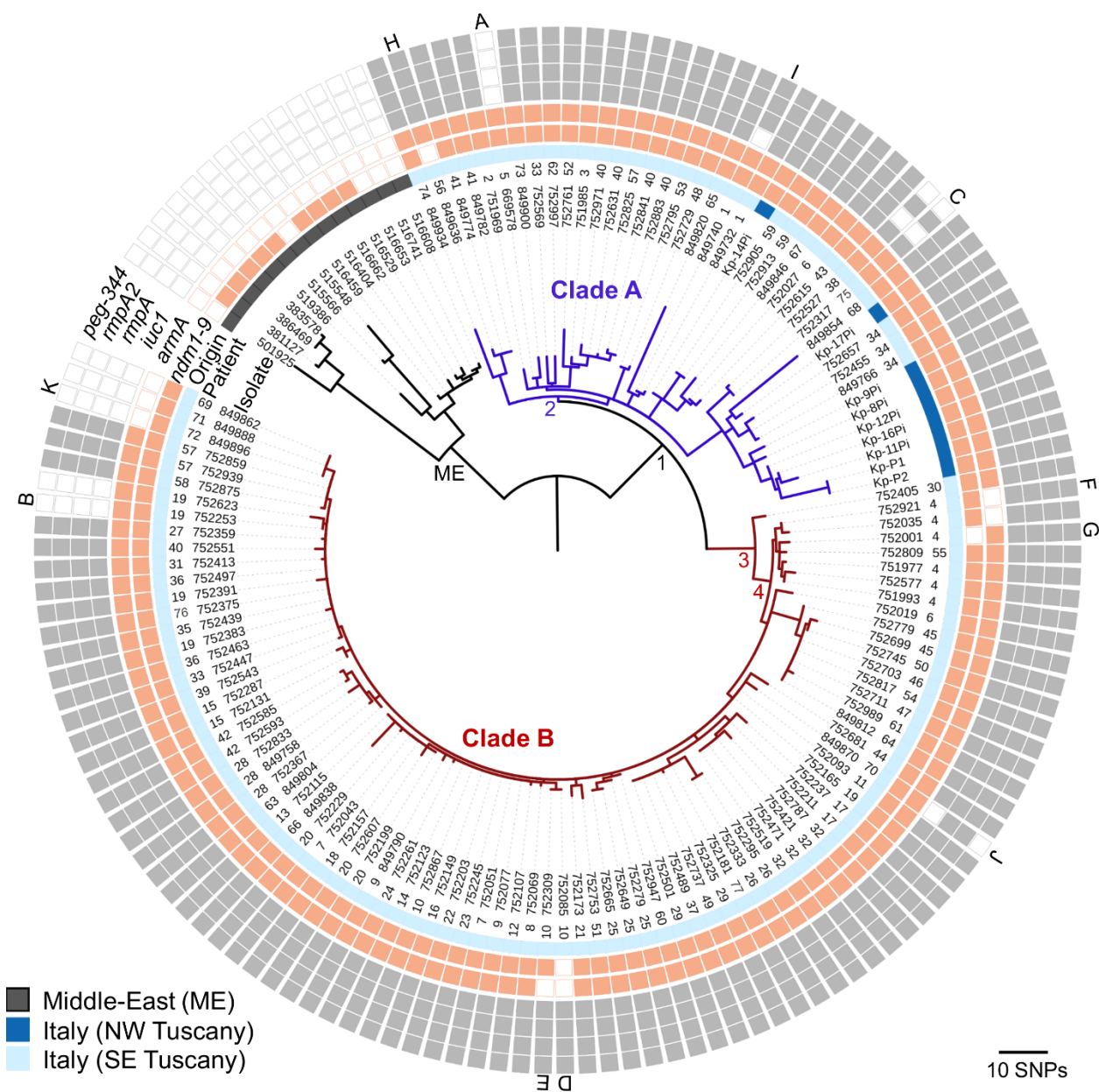560   *Nucleic Acids Research* **47**, W256–W259 (2019).

561

Figure 1. Maximum likelihood core SNP-based phylogeny of *K. pneumoniae* ST-147 from Italy. Closely related isolates from the Middle East were included as an outgroup. Nodes of interest (all with bootstrap values > 80) are labeled (ME, 1 to 4). When available, numerical patient identifiers are provided (1 to 77). Concentric rings indicate the presence (closed symbol) of a selection of plasmid-bound resistance and virulence genes. Apparent variations in plasmid content are labeled (A to K) on the outermost ring.
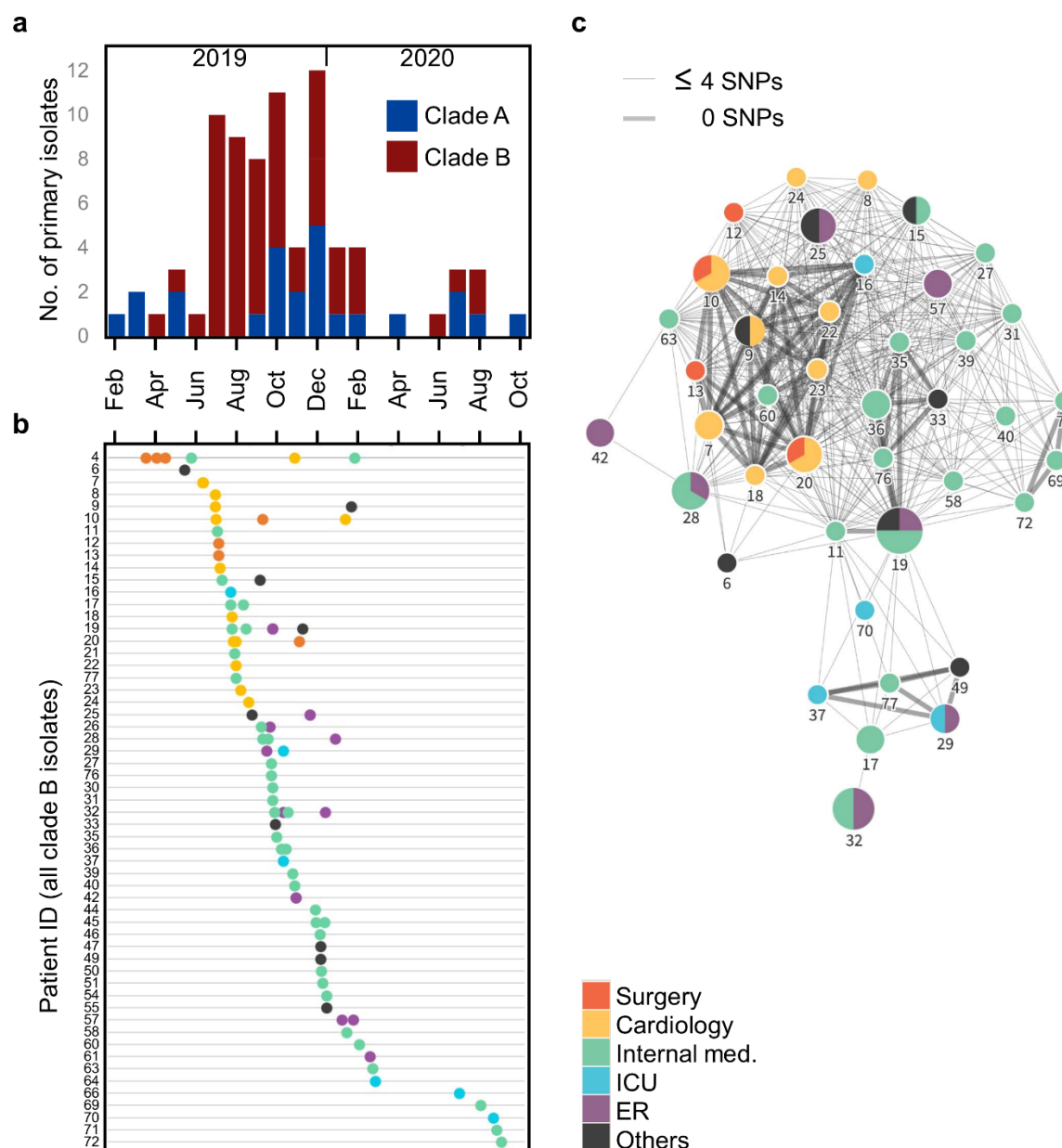
Fig. 2. **Rapid, nosocomial spread of Clade B ST-147 clone. (A)** Epidemic curve of all patient's first isolate (i.e. no serial isolates) collected in SE Tuscany and colored by phylogenetic clade (A or B). **(B)** Patient charts showing the date (x-axis) and location (colored legend) of all first and serial clade B isolates (dots). **(C)** Network of patients with near-identical clade B isolates (≤4 SNPs). Nodes are labeled with their respective patient ID and indicate the location (colored pie chart) and number (size) of serial isolates.

28
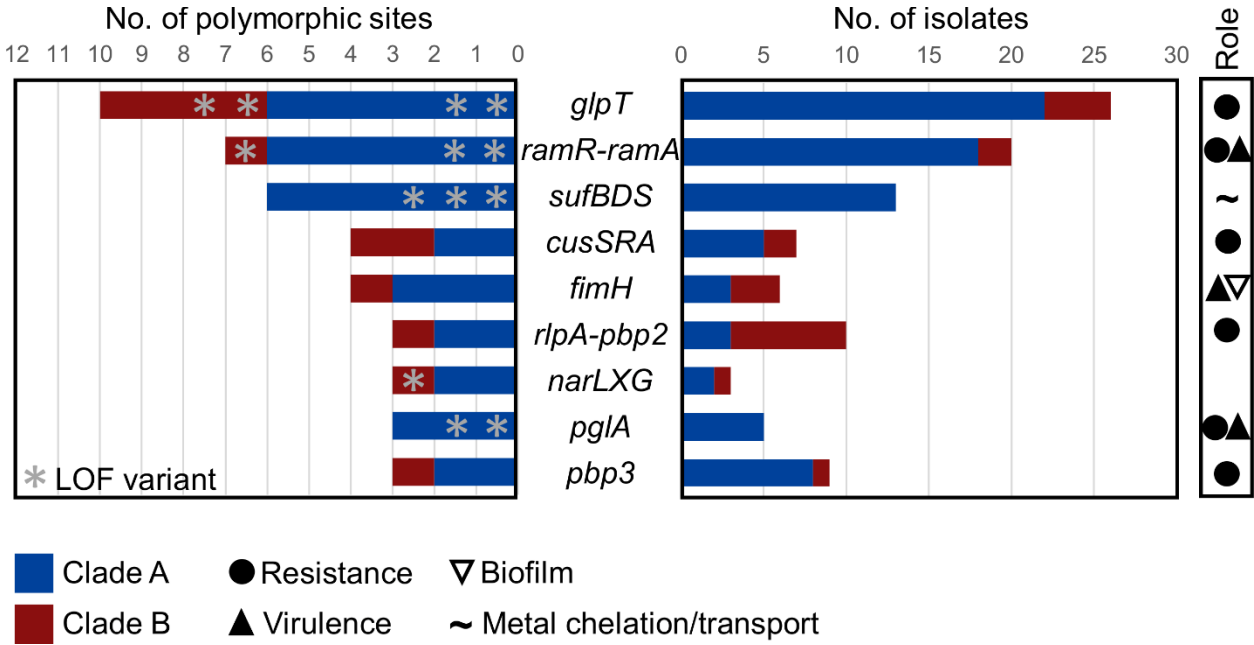
Fig. 3. Convergent evolution on resistance and virulence genes. List of genes (or functional clusters of syntenic genes) that were repeatedly and independently (3 or more) mutated among the outbreak isolates. Bars show the number of different mutations within each gene or functional cluster (left diagram) and the numbers of isolates with a mutated allele (right diagram). Data is plotted for isolates from both phylogenetic clades. When available, and based on the literature, the role of genes and functional clusters in relevant phenotypes is indicated.

584
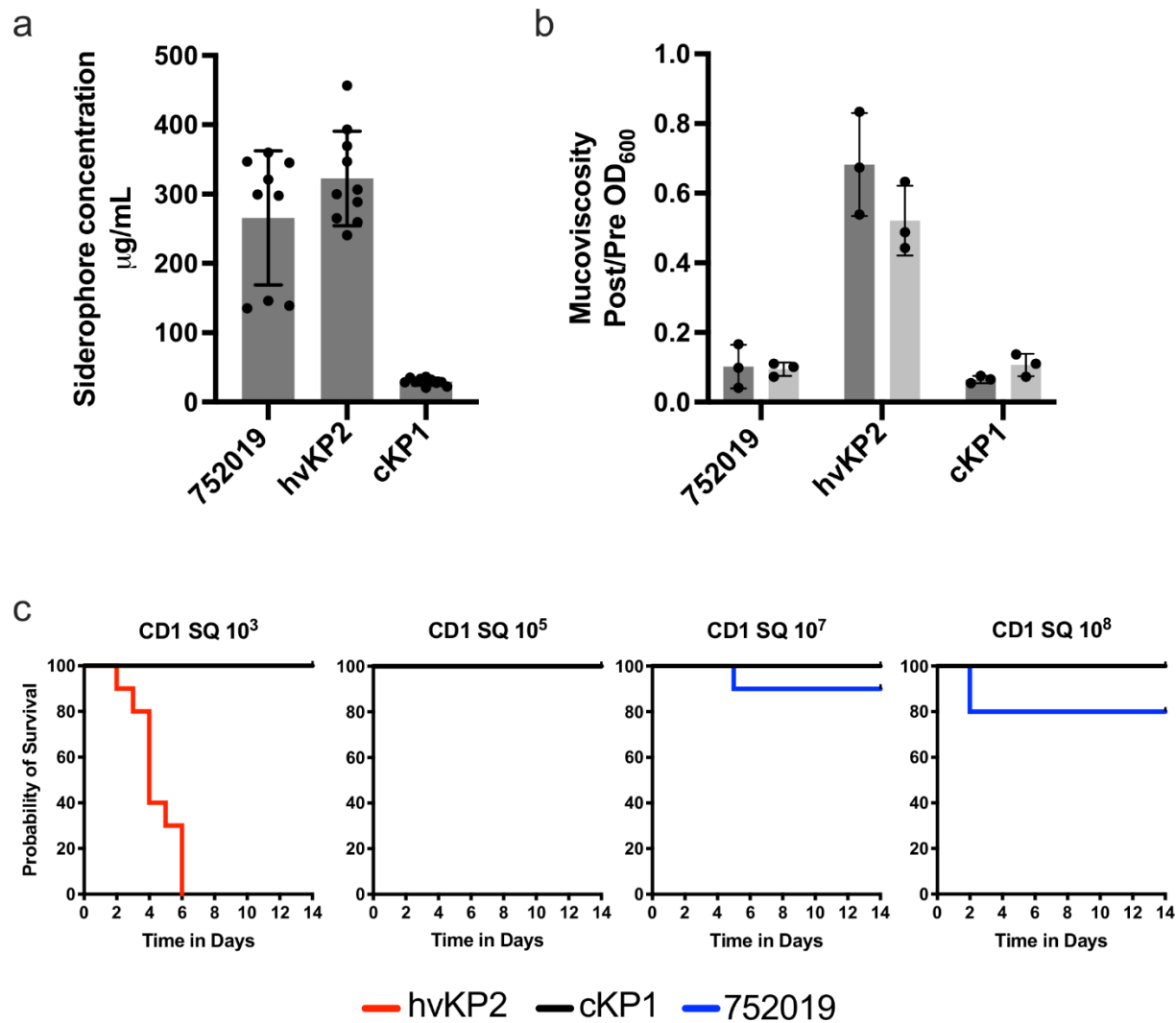
Fig. 4. Pathogenicity of the convergent ST-147 clone from Italy. **(A)** Quantitative siderophore production of outbreak isolate 752019 carrying the canonical pSI0739-ARMA-Vir. Reference strains hvKP2 (hypervirulent pathotype) and cKP1 (classical pathotype) are shown throughout all panels for comparison. **(B)** Mean mucoviscosity of outbreak isolate 752019 compared to reference *K. pneumoniae* isolates. Independent assays were performed for both media (LB and M9). **(C)** Kaplan-Meier survival curves of outbred CD1 mice after subcutaneous (SQ) challenge with 10^3, 10^5, 10^7, or 10^8 CFU of outbreak isolate 752019 or reference isolates hvKP2 and cKP1. Total *n*=10 (*n*=5 in each of 2 independent experiments) for each titer for each strain.

593   **Supplemental information**

594   **Table S1.** Characteristics of all isolates used in this study.

595   **Table S2.** Antibiotic susceptibility profiles for a selection of ST-147 isolates.

596   **Table S3.** Overview of plasmid relatedness with pSI0739-ARMA-Vir. .

597   **Table S4.** List of predicted variants in ST-147 isolates used in this study.
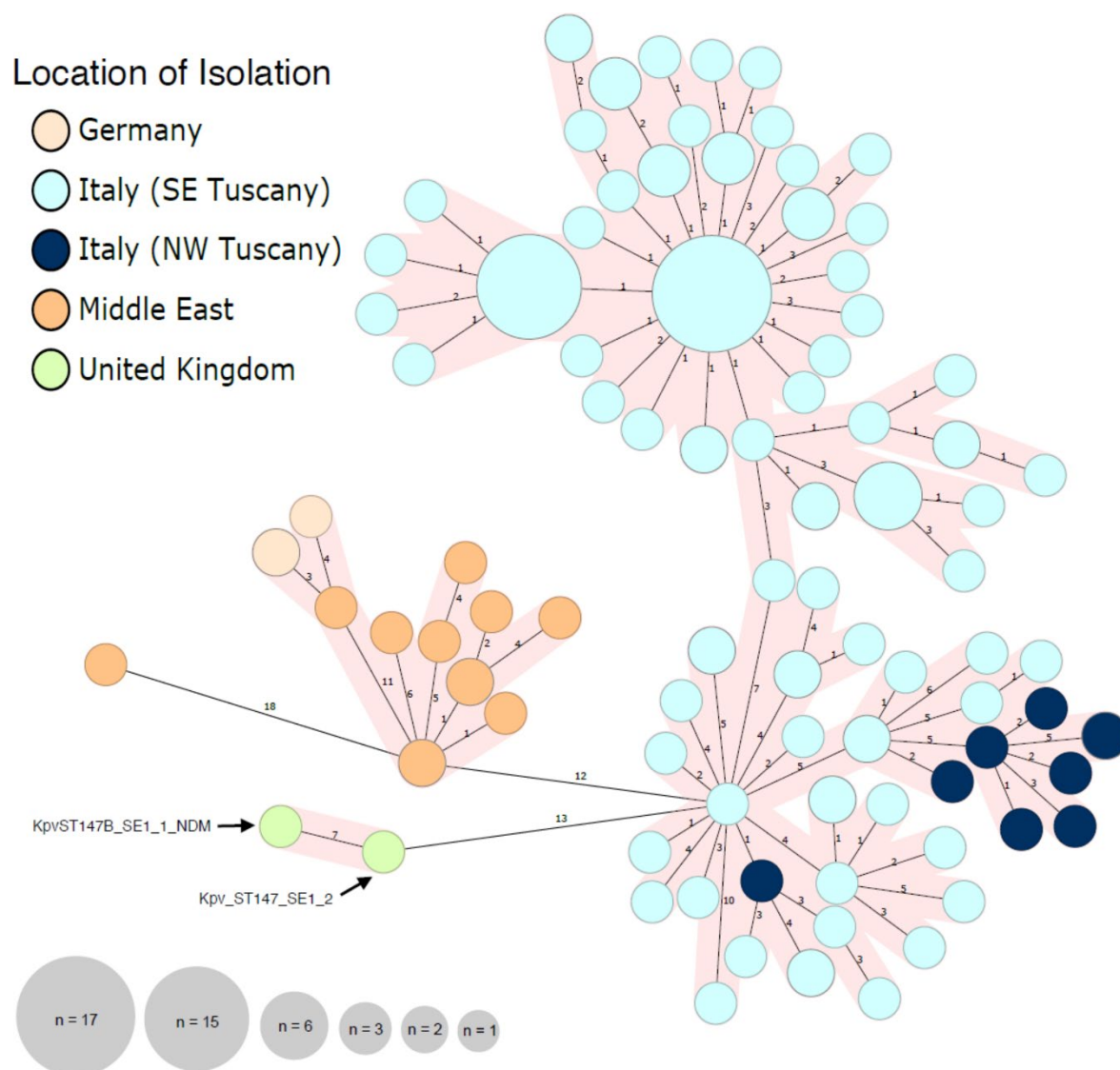
598

Figure S1. cgMLST minimum spanning tree of 143 ST-147 *K. pneumoniae* genomes used to determine the genetic relatedness of the Italy ST-147 outbreak clone to available ST-147 genomes from the MRSN collection and public databases. cgMLST allelic profiles are represented by circles, and circle sizes are proportional to the number of isolates sharing that profile. The line length connection the isolates represents the number of allelic differences between each profile. Isolates with 11 or less allelic differences are highlighted with pink shading around them.

a

b

607
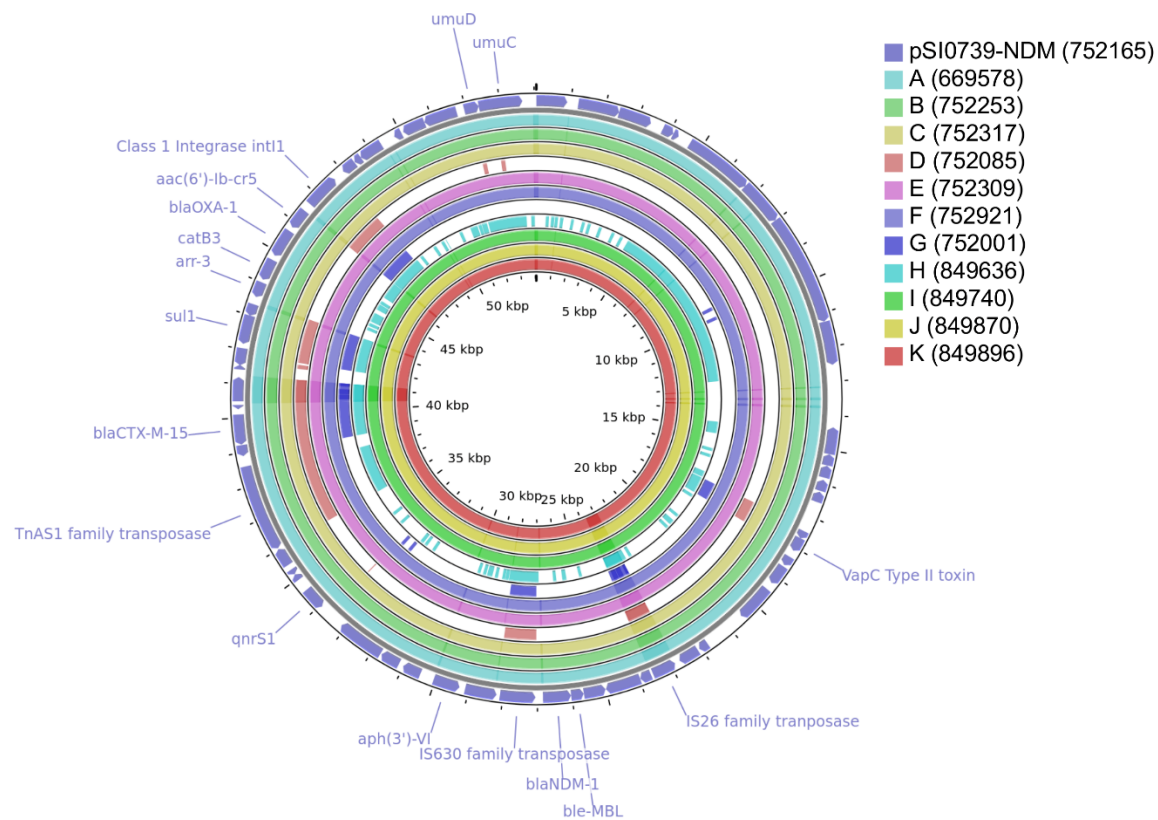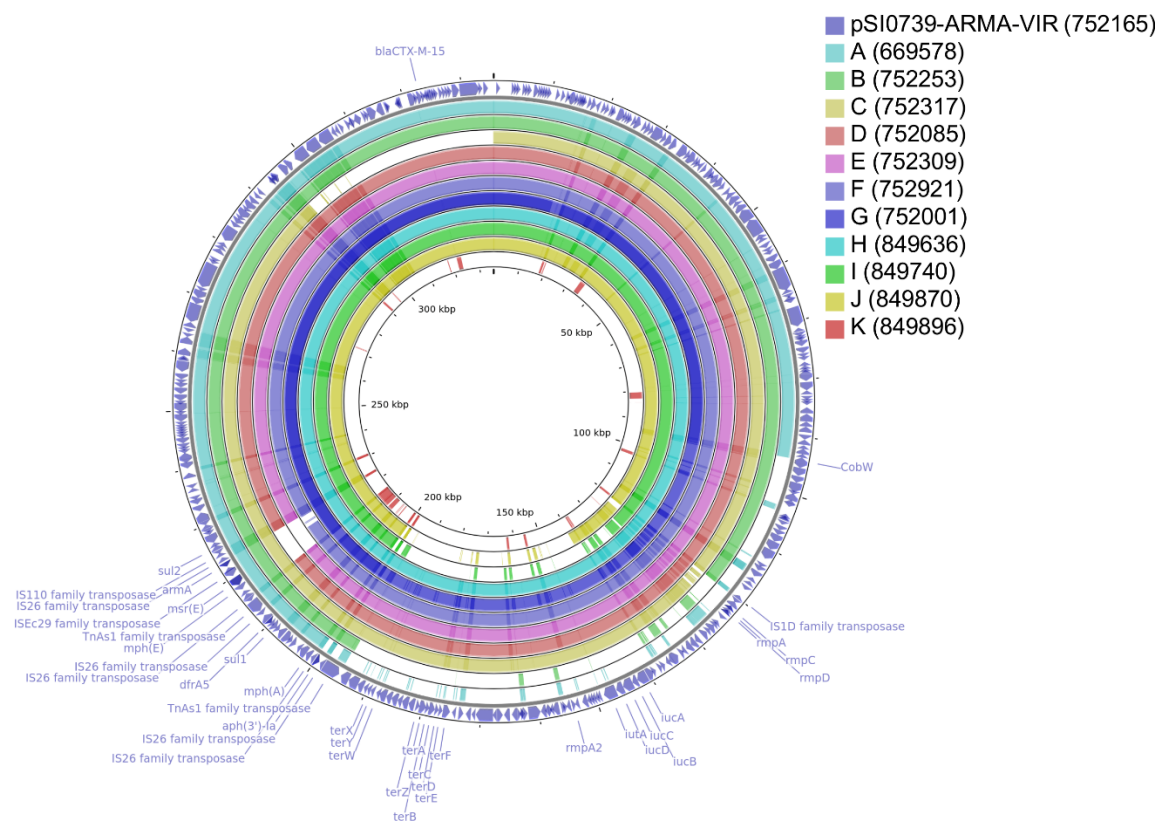
608 **Figure S2**. Sequence similarity of hybrid plasmid types identified in this study. **(A)** Sequence

609 assembly contigs from each isolate were blasted against the closed ST-147 NDM carrying

610 plasmid from this study, pSI0739-NDM and **(B)** the hybrid plasmid pSI0739-ARMA-Vir from

611 this study. For each panel, the outer ring represents the reference plasmid. Inner rings represent

612 predicted excision events or plasmid loss identified in a selection (labeled A-K) of outbreak
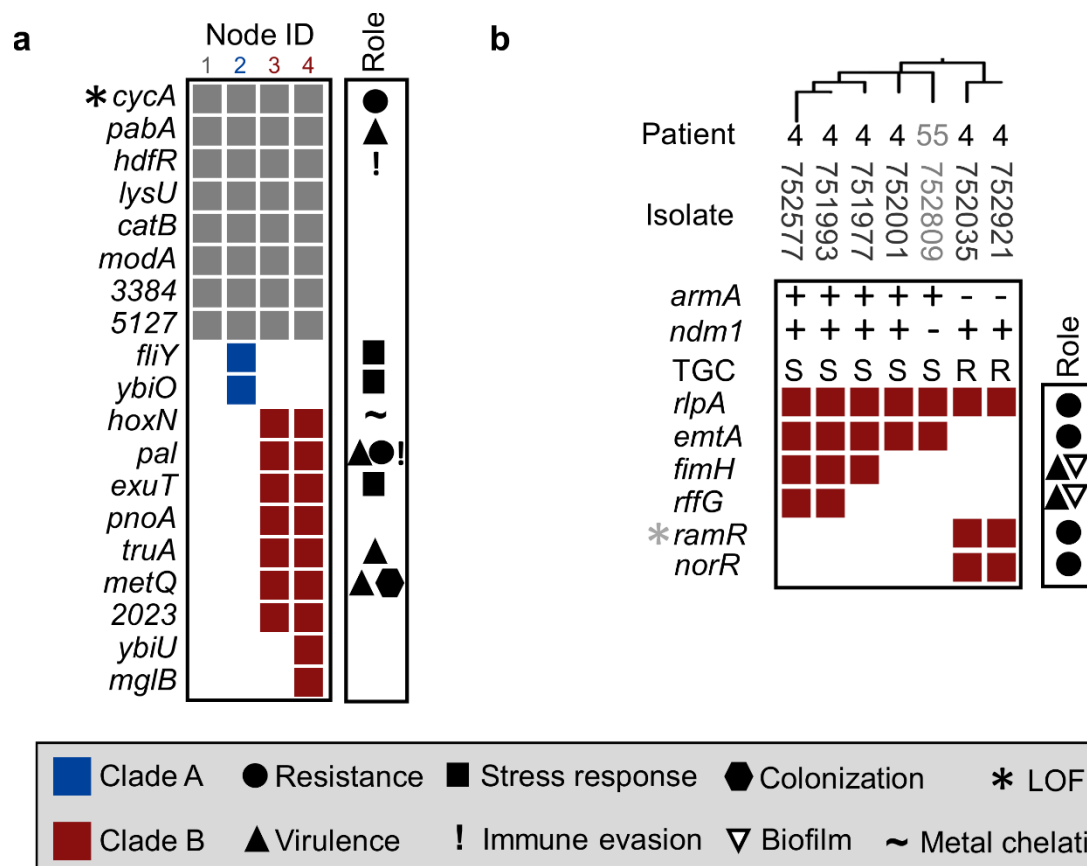
613 isolates.

614

Figure S3. (A) Fixation of shared variants within the *K. pneumoniae* ST-147 outbreak strains (nodes 1-4 corresponding to Fig. 1). **(B)** Stepwise, fixation of variants found in 6 serial isolates from patient 4, clade B. For each gene, based on analysis of the literature, the role of its corresponding protein in resistance, virulence, metal transport, or biofilm formation is indicated.
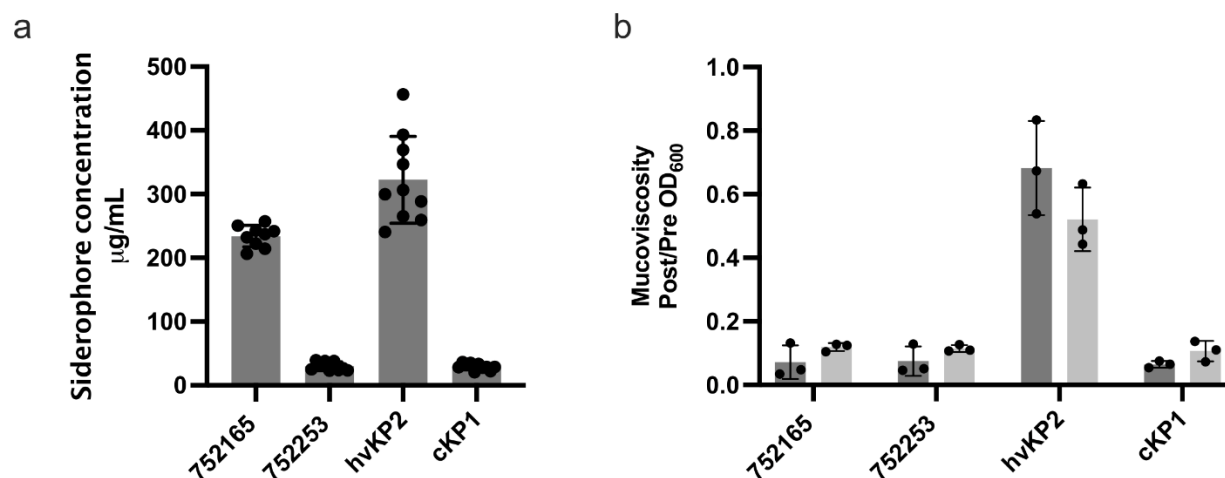
35

621

Figure S4. (A) Quantitative siderophore production of outbreak isolates 752165 (pSI0739-ARMA-Vir) and 752253 (pSI0739-ARMA-Vir, event B). **(B)** Mean mucoviscosity of outbreak isolates 752165 and 752253 compared to reference *K. pneumoniae* isolates. Independent assays were performed for both media (LB and M9). Reference hypervirulent (hvKP2) and "classical" (cKP1) isolates are shown throughout all panels for comparison.
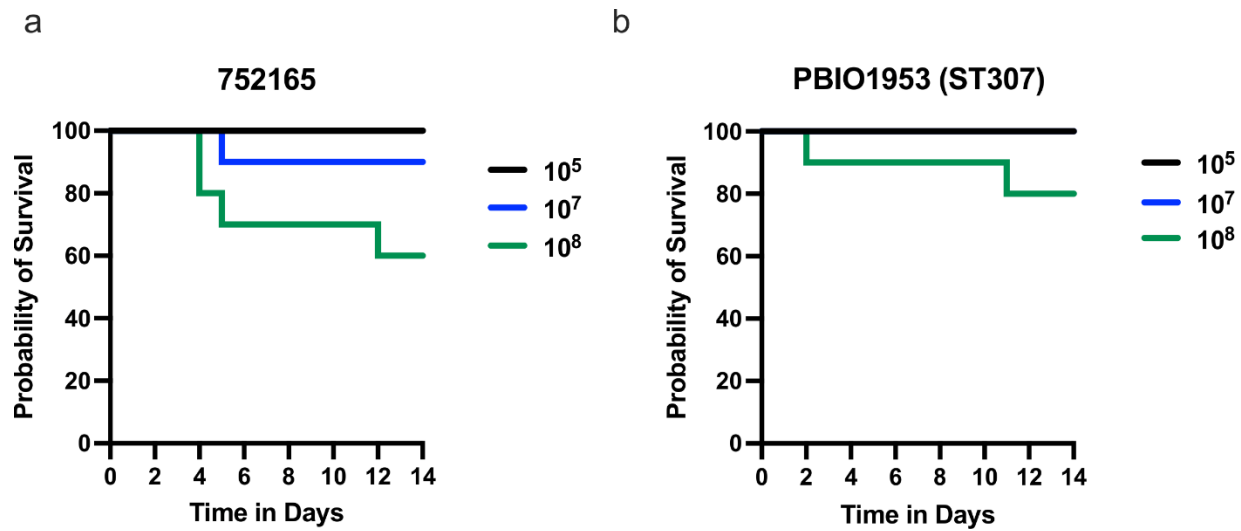
627

Fig. S5. Kaplan-Meier survival curves of outbred CD1 mice after subcutaneous (SQ) challenge with 10^5, 10^7, or 10^8 CFU of **(A)** outbreak isolate 752165 and **(B)** ST307 strain PBIO1953. Total n=10 (n=5 in each of 2 independent experiments) for each titer for each strain.